

# Diagnosis of Intense Pulsed Aluminium Ion Beam by Magnetically Insulated Ion Diode

Hiroaki ITO, Kodai FUJIKAWA and Katsumi MASUGATA

*Dep. of Electrical and Electronic Engineering, University of Toyama, 3190 Gofuku, Toyama 930-8555, Japan*

(Received: 24 August 2008 / Accepted: 6 December 2008)

Intense pulsed heavy ion beam is expected to be applied to materials processing including surface modification and ion implantation. For those applications, it is very important to generate high-purity pulsed ion beams with various ion species. A magnetically insulated ion diode with an ion source of a vacuum arc plasma gun has been developed in order to generate pulsed metallic ion beams. When the ion diode was operated at diode voltage  $\approx 200$  kV, diode current  $\approx 15$  kA and pulse duration  $\approx 100$  ns, the ion beam with an ion current density of  $> 200$  A/cm<sup>2</sup> was obtained at 50 mm downstream from the anode. From the evaluation of the energy and ion species by Thomson parabola spectrometer, the ion beam consists of aluminium ions (Al<sup>+</sup>, Al<sup>2+</sup> and Al<sup>3+</sup>) of energy 60-740 keV and the proton impurities of energy 90-150 keV. The purity of the beam was estimated to be 89 %.

Keywords: pulsed heavy ion beam, magnetically insulated ion diode, vacuum arc plasma gun, pulsed power technology

## 1. Introduction

High-intensity pulsed heavy ion beam (PHIB) technology has been developed over the last two decades primarily for nuclear fusion and high energy density physics research [1, 2]. One of most interesting topics is the application of pulsed heavy ion beam as a tool for material processes including the surface modification, thin film deposition and ion implantation [3-5]. Especially for the ion implantation process to semiconductor materials for the next generation including silicon carbide and diamond, the pulsed heavy ion beam technique has received extensive attention as a new ion implantation technology named "pulsed ion beam implantation", since the ion implantation and the surface heat treatment or the surface annealing can be completed in the same time [6].

The pulsed ion beams usually are generated in conventional magnetically insulated ion diodes (MID) with transverse magnetic field in the acceleration gap to suppress the electron flow and enhance the ion flow. The purity of the pulsed ion beam, however, is usually deteriorated by absorbed matter on the anode (flash-board) surface and residual gas molecules in the diode chamber, since the surface flashover ion source is used for the ion source of the MID. For example, the pulsed heavy ion beam produced in a point pinch ion diode contains many kinds of ions including protons, multiply ionized carbons, and organic ions [7]. In addition, the producible ion species are limited to the material of electrode (anode). Therefore, the conventional pulsed ion diode is not suitable for the application of the pulsed heavy ion beam to the ion implantation.

It is very important for the ion implantation to develop the accelerator technology to generate high-

purity ion beams with various ion species. In order to produce the pulsed heavy ion beam with various ion species for material processes, we have developed a new type of MID with an ion source of a gas puff plasma gun [8]. When the ion diode was operated at a diode voltage of about 190 kV, a diode current of about 15 kA, and a pulse duration of 100 ns (FWHM), the nitrogen ion beam with an ion current density of 54 A/cm<sup>2</sup> and a pulse duration of 90 ns was successfully obtained at 50 mm downstream from the anode. We found from Thomson parabola spectrometer that the ion beam consisted of N<sup>+</sup> and N<sup>2+</sup> beam with energy of 100-400 keV and impurity of proton with energy of 90-200 keV. The purity of the nitrogen beam was estimated to be 94 % [9].

The magnetically insulated ion diode using the gas puff plasma gun as the ion source enabled us to generate intense pulsed gaseous ion beams, but there has been an increasing demand for pulsed metallic ion beams for the materials processing. Metal vapor vacuum ion source is suitable for the production of high-current metallic ion beams [10]. In order to generate a variety of metallic ion beam, we have developed the magnetically insulated ion diode with an ion source of the vacuum arc plasma gun. In this paper, we present the evaluation of the properties of the pulsed ion beam.

## 2. Experimental Setup

A schematic configuration of the intense pulsed heavy ion diode system is illustrated in Fig. 1. The system consists of a high voltage pulsed power generator, an ion source, a B<sub>y</sub> type magnetically insulated ion acceleration gap (diode), and a stainless-steel vacuum chamber with a diffusion pump package. The Marx generator with the stored energy of 240 J at a

author's e-mail: hiroaki@eng.u-toyama.ac.jp

charging voltage 50 kV is used as the pulsed power generator of the ion diode. The output parameters of the Marx generator are voltage 200 kV, current 15 kA and pulse duration 100 ns(FWHM), which is applied to the anode of the ion diode. The ion source is installed inside the anode. The vacuum chamber is evacuated to  $5 \times 10^{-3}$  Pa.

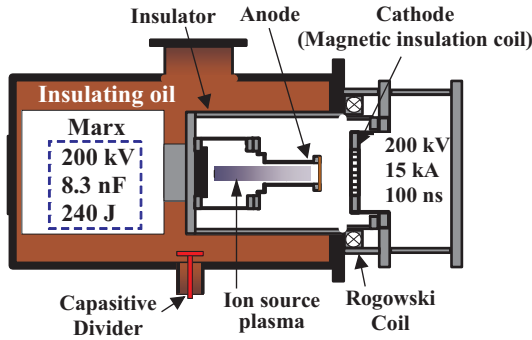


Fig. 1 Schematic of the Ion Diode System.

Figure 2 shows the cross-sectional view of  $B_y$  type ion diode. The ion diode consists of a cylindrical anode of 115 mm length by 60 mm diameter and a cathode of grid structure. The acceleration gap length ( $d_{A-K}$ ) is adjusted to 10 mm. The top of the anode is a stainless-steel plate, in which a hole of 30 mm diameter is drilled at the central area of the anode in order to allow the source plasma to inject into the acceleration gap. The cathode has a grid structure to pass through the accelerated ions. The cathode also acts as a multi-turn magnetic field coil in order to generate a transverse magnetic field in the acceleration gap to insulate the electron flow and enhance the ion flow. Thus, as shown in Fig. 2, the cathode (coil) has a shape like 8-character and is made of phosphor bronze strip of 10 mm width and 1 mm thickness. The coil is powered by a capacitor bank of 250  $\mu$ F and charging voltage 3 kV. By applying a pulse current of 10 kA with rise-time 50  $\mu$ s, a uniform magnetic field of 0.7 T is produced in the acceleration gap.

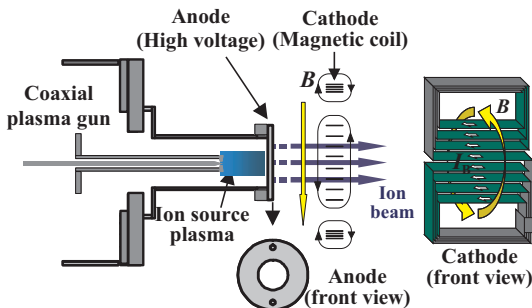


Fig. 2 Cross-sectional view of  $B_y$  type magnetically insulated acceleration gap.

A vacuum arc plasma gun is employed as the ion source of MID to produce the metallic ion source plasma. The metallic plasma is produced by an

ionization of cathode materials evaporated from cathodic spots of the vacuum arc discharge. Thus, high amounts of metallic ions can be achieved. Figure 3 shows the design of the plasma gun and the experimental setup to evaluate the characteristics of the plasma gun. As shown in Fig. 3, the plasma gun has a pair of coaxial aluminium electrodes, i.e., an inner electrode of 200 mm length by 6 mm outer diameter and an outer electrode of 10 mm inner diameter. On the top of outer electrode the gap length is reduced to 1 mm. A capacitor bank of 3.3  $\mu$ F for the plasma gun is charged up to 30 kV. The capacitor bank is connected anode to cathode and is triggered by applying 15 kV spark between the cathode and the trigger electrode of the field-distortion switch. The pulsed current by the capacitor bank is fed through inductively coupled coaxial cables, since the plasma gun is placed inside the anode where the high-voltage pulse is applied. The ion current density of the plasma ( $J_i$ ) produced by the plasma gun was evaluated by a biased ion collector placed on the central axis at  $z = 50$  mm downstream from the top of the plasma gun where the anode is placed in the acceleration experiment.

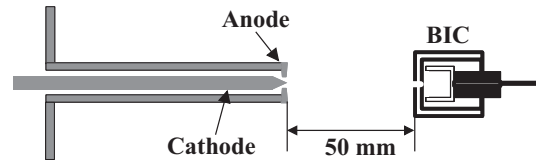


Fig. 3 Design of vacuum arc ion source and experimental setup to evaluate ion current density.

Figure 4 shows the typical waveforms of the discharge current ( $I_p$ ) and the ion current density ( $J_i$ ). As seen in Fig. 4, the discharge current  $I_p$  has a sinusoidal waveform of peak current 12 kA and quarter cycle 6  $\mu$ s. The ion beam with a peak current density  $J_i=158$  A/cm<sup>2</sup> and a pulse duration of 2.5  $\mu$ s is observed at about  $\tau_p = 7.5$   $\mu$ s after the rise of  $I_p$ . This result suggests that it takes 7.5  $\mu$ s for the ion beam produced in the plasma gun to reach the acceleration gap. Assuming that the plasma is produced at the rise of  $I_p$ , the delay time between  $I_p$  and  $J_i$  gives the drift velocity of  $6.7 \times 10^3$  m/s, which corresponds to

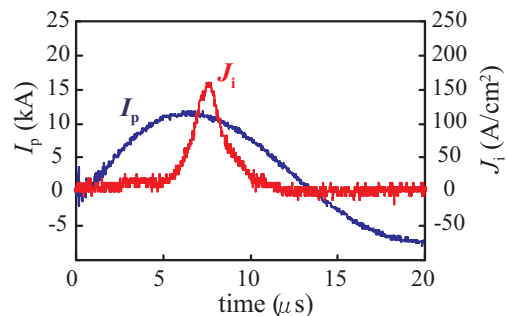


Fig. 4 Typical waveforms of discharge current  $I_p$  and ion current density  $J_i$  of the plasma gun.

the ion energy of 6 eV.

### 3. Experimental Results

Figure 5 shows the typical waveforms of the diode voltage ( $V_d$ ), the diode current ( $I_d$ ) and the ion current density of the accelerated ion beam ( $J_i$ ). Here, the Marx generator was charged up to 50 kV and fired at a delay time of  $\tau_d=7.5 \mu\text{s}$  after the rise of the discharge current of the plasma gun. The ion-beam current density  $J_i$  is measured by the BIC (biased ion collector) placed at  $z = 50 \text{ mm}$  downstream from the surface of the anode on the axis. As seen in the Fig. 5(a),  $V_d$  rises in 50 ns and has a peak of 220 kV, whereas  $I_d$  rises with  $V_d$  and has a peak of 12 kA at  $t = 75 \text{ ns}$ . It can be clearly seen from Fig. 5(b) that the ion beam of the ion current density  $J_i = 230 \text{ A/cm}^2$  and pulse duration 40 ns (FWHM) is obtained at 45 ns after the peak of  $V_d$ . Considering the time of flight delay, the ion beam corresponding the peak of  $J_i$  seems to be accelerated around the peak of  $V_d$ .

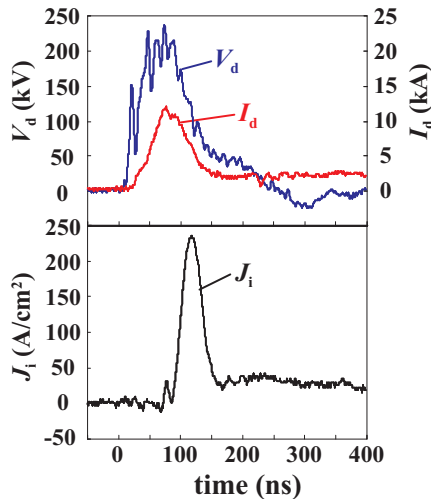


Fig. 5 Typical waveforms of (a) diode voltage  $V_d$ , diode current  $I_d$  and (b) ion-beam current density  $J_i$ .

In order to evaluate the ion species and the energy spectrum of the ion beam, the Thomson parabola spectrometer (TPS) [11] was used. The TPS consists of a 1st pinhole, a 2nd pinhole, a magnetic deflector, an electric deflector and an ion detecting plate of CR-39. Figure 6 illustrates an example of the track pattern recorded on the CR-39 ion track detecting plate. Here,  $Z$  in Fig. 6 is the charge state of ions. Data from up to 5 shots are taken on one CR-39 detector to average shot-to-shot variations. The deflecting magnetic field of 0.8 T and the electric field of 0.6 MV/m are applied in the vertical direction. Hence, ions are deflected in the vertical direction and the horizontal direction by the electric field and the magnetic field, respectively. We can evaluate the ion number ratio on each ion species by counting the track number, since each ion track on CR-39 is produced by an irradiation of single ion. The energy range and the number ratio

of each ion species evaluated from the track pattern are summarized in Table 1. It is clearly seen that the ion beam consists of  $\text{Al}^+$ ,  $\text{Al}^{2+}$  and  $\text{Al}^{3+}$  beam with an energy of 60-740 keV and impurity of proton with an energy of 90-150 keV. The high-energy end of the traces of aluminum ions is around  $250 \text{ keV}/Z$ , which coincides with the peak value of acceleration voltage ( $V_d \approx 220 \text{ kV}$ ). We see from the table that 11 % of impurity ions of protons are included in the beam, hence the purity of the beam is evaluated to be 89 %. These results show clearly that the pulsed aluminium ion beam is successfully obtained by the magnetically insulated ion diode with the vacuum arc plasma gun.

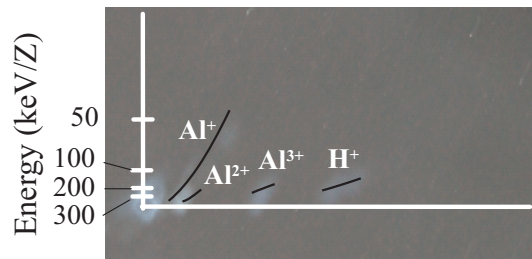


Fig. 6 Typical ion track pattern on CR-39 obtained by TPS.

Table.1 Energy and number ratio of each ion species evaluated by TPS.

Ion species	Energy (keV)	Number ratio (%)
$\text{Al}^+$	60-240	89
$\text{Al}^{2+}$	240-510	
$\text{Al}^{3+}$	480-740	
$\text{H}^+$	90-150	11

Figure 7(a) shows the dependence of the ion beam current density of the ion diode ( $J_i$ ) on the shot number. The experimental parameters are the same as those mentioned previously in this paper. As seen in Fig. 7(a), the accelerated ion-beam current density  $J_i$  is poorly reproducible and ranges from 0 to  $260 \text{ A/cm}^2$ . The average value of  $J_i$  in 40 shots is calculated to be  $108 \text{ A/cm}^2$ . In order to find out the reason

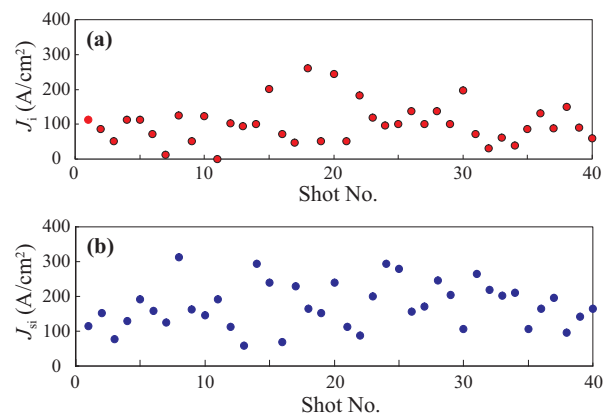


Fig. 7 Dependence of (a) accelerated ion-beam current density  $J_i$  and (b) ion current density of source plasma  $J_{si}$  on shot number.

of the shot-to-shot fluctuation of  $J_i$ , the reproducibility of the ion current density of the vacuum arc plasma gun ( $J_{si}$ ) was evaluated. The experimental results are displayed in Fig. 7(b). It is clearly seen from Fig. 7(b) that there is a lot of scatter in the ion current density of the plasma gun and the reproducibility of  $J_{si}$  is very poor. The ion current density  $J_{si}$  ranges from 20 to 300 A/cm<sup>2</sup> and the average value of  $J_{si}$  in 40 shot is calculated to be 174 A/cm<sup>2</sup>. It is thought that the poor reproducibility of the accelerated ion-beam current density is caused by the shot-to-shot fluctuation of the plasma source produced in the plasma gun.

In order to evaluate the spatial uniformity of the aluminium ion beam current density, we used five BICs arrayed at positions shown in Fig. 8. With five BICs, we obtained the azimuthal distribution of the ion-beam current density on planes perpendicular to the central axis. The experimental results are displayed in Fig. 9(a). Here, each data point in Fig. 9(a) is an average of five ion beam shots. Although the ion-beam current density  $J_i$  at each position has a lot of scatter, we see that the ion-beam current density on the side of BIC3 is much larger than that on the opposite side (BIC5). This fluctuation is caused by the poor reproducibility of the ion beam.

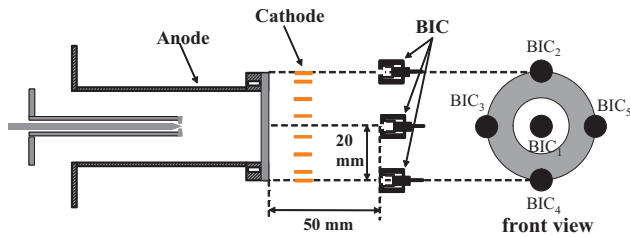


Fig. 8 Experimental setup for measurement of radial distribution of ion-beam current density.

Figure 9(b) shows the damage pattern of the ion beam recorded on the thermo-sensitive paper to measure the cross-sectional distribution of the ion-beam current density. Here, thermo-sensitive paper was placed at  $z = 50$  mm downstream from the anode. It is evident from Fig. 9(b) that the ion beam tends to shift to the direction of  $E \times B$  drift. Positions of each BIC are shown in the figure as the reference. The azimuthal distribution of the ion beam is in fairly good agreement with the result observed in Fig. 9(a).

#### 4. Conclusion

We have developed the magnetically insulated ion diode with an ion source of a vacuum arc plasma gun in order to generate the pulsed metallic ion beam. When the ion diode was operated at a diode voltage of about 220 kV, a diode current of about 12 kA and a pulse duration of 100 ns, the aluminium ion beam with an ion current density of about 230 A/cm<sup>2</sup> and a pulse duration of 40 ns was obtained at 50 mm down-

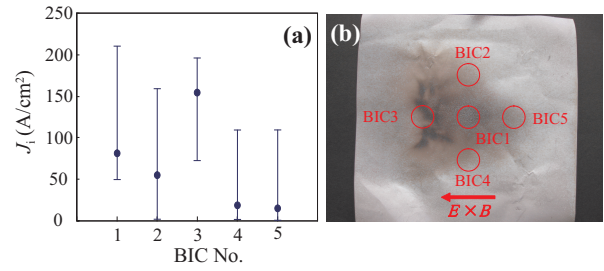


Fig. 9 (a) Spatial distribution of ion current density.(b) Damage pattern of ion beam recorded on thermo-sensitive paper.

stream from the anode. The energy and ion species of the ion beam were evaluated by the Thomson parabola spectrometer and we found that aluminium ions ( $Al^+$ ,  $Al^{2+}$  and  $Al^{3+}$ ) of energy 60-740 keV were accelerated with impurity proton of energy 90-150 keV. The purity of the aluminium ion beam was estimated to be 89 %. It is possible to generate a wide variety of pulsed ion beam by using two types of plasma gun as the ion source, i.e., a gas puff plasma gun and a vacuum arc plasma gun. However, there seems to be some room for making improvements including the purity and the shot-to-shot reproducibility of the ion beam to apply the pulsed heavy ion beam to the ion implantation.

#### Acknowledgement

This work is supported in part by the Grant-in-Aid for Scientific Research from the Ministry of Education, Science, Sports and Culture, Japan.

- [1] J.P. VanDevender and D.L. Cook, *Science* **232**, 831 (1986).
- [2] S. Kawata, K. Horiaka, M. Murakami, *et al.*, *Nucl. Instrum. & Methods in Phys. Res. A* **577**, 21 (2007).
- [3] K. Yatsui, X. D. Kang, T. Sonogawa, T. Matsuoka, K. Masugata, Y. Shimotori, T. Satoh, *et al.*, *Phys. Plasmas* **1**, 1730 (1994).
- [4] A. N. Valyaev, V. S. Ladysev, D. R. Mendygaliyev, A. D. Pogrebnyak, A. A. Valyaev and N. A. Pogrebnyak, *Nuclear Instrum. Methods in Phys. Res. B* **171**, 481 (2000).
- [5] A. D. Korotaev, A. N. Tyumentsev, Yu. P. Pinzhin and G. E. Remnev, *Suf. Coat. Technol.* **185**, 38 (2004).
- [6] K. Masugata, *et al.*, *Proc. 25th Int. Power Modulator Symposium*, 2002 (Hollywood, CA, USA, 2002) pp.552-555.
- [7] Y. Hashimoto, M. Yatsuzuka, and S. Nobuhara, *Jpn. J. Appl. Phys.* **32**, 4838 (1993).
- [8] K. Masugata, R. Tejima, M. Higashiyama, J. Kawai, I. Kitamura, H. Tanoue and K. Arai, *Plasma Device and Operations* **13**, 57 (2005).
- [9] K. Masugata, H. Ito, H. Miyake and L. Wang, *Proc. 2007 IEEE Pulsed Power and Plasma Science Conference*, (Albuquerque, NM, USA, 2007), pp.835-838.
- [10] I. Brown, *Rev. Sci. Instrum.* **65**, 3061 (1994).
- [11] M. J. Rhee, *Rev. Sci. Instrum.* **55**, 1229 (1984).